Green Chemistry

Accepted Manuscript

This article can be cited before page numbers have been issued, to do this please use: X. Yang, J. Bian, J. Huang, W. Xin, T. Lu, C. chen, Y. Su, Z. Lipeng, F. Wang and J. Xu, *Green Chem.*, 2016, DOI: 10.1039/C6GC02437H.

This is an Accepted Manuscript, which has been through the Royal Society of Chemistry peer review process and has been accepted for publication.

Accepted Manuscripts are published online shortly after acceptance, before technical editing, formatting and proof reading. Using this free service, authors can make their results available to the community, in citable form, before we publish the edited article. We will replace this Accepted Manuscript with the edited and formatted Advance Article as soon as it is available.

You can find more information about Accepted Manuscripts in the author guidelines.

Please note that technical editing may introduce minor changes to the text and/or graphics, which may alter content. The journal's standard Terms & Conditions and the ethical guidelines, outlined in our author and reviewer resource centre, still apply. In no event shall the Royal Society of Chemistry be held responsible for any errors or omissions in this Accepted Manuscript or any consequences arising from the use of any information it contains.

ROYAL SOCIETY OF CHEMISTRY

rsc.li/green-chem

View Article Online
DOI: 10.1039/C6GC02437H

Fluoride-free and low concentration template synthesis of hierarchical Sn-Beta zeolites: efficient catalyst for conversion of glucose to alkyl lactate

Xiaomei Yang,[a] Jingjing Bian,[a] Jianhao Huang,[a] Weiwen Xin,[a] Tianliang Lu,[b] Chen Chen,[c] Yunlai Su,[a] Lipeng Zhou,[a,*] Feng Wang,[c] Jie Xu[c]

[a] *College of Chemistry and Molecular Engineering, Zhengzhou University, 100 Kexue Road, Zhengzhou 450001, China*

[b] *School of Chemical Engineering and Energy, Zhengzhou University, 100 Kexue Road, Zhengzhou 450001, China*

[c] *State Key Laboratory of Catalysis, Dalian National Laboratory for Clean Energy, Dalian Institute of Chemical Physics, Chinese Academy of Sciences, 457 Zhongshan Road, Dalian 116023, China*

* Corresponding author. Tel.: +86 371 67781780; fax: +86 371 67766076. *E-mail addresses:* zhoulipeng@zzu.edu.cn

View Article Online
DOI: 10.1039/C6GC02437H

Abstract

Hierarchical Sn-Beta zeolite was prepared through a hydrothermal postsynthesis method, which employed no fluoride and only a small amount of tetraethyl ammonium hydroxide (TEAOH). The dual roles of TEAOH as a base and as a structure directing agent were discussed in detail, which were significantly affected by its concentration. At TEAOH concentration of 0.2~0.4 mol L^{-1}, hierarchical Sn-Beta zeolites with the most probable mesopores of 7.8 nm were achieved. Other physicochemical properties of the hierarchical Sn-Beta including the content and state of Sn and the acidity were also characterized. The hierarchical Sn-Beta zeolite gave higher yield of methyl lactate (58%) than the microporous Sn-Beta zeolite synthesized in fluoride medium (47%) due to the promotion effect of the hierarchical porosity for the conversion of glucose in methanol, which is an important and challenging process of biorefinery. The hierarchical Sn-Beta zeolite is stable and can be recycled and reused five times without significant loss of activity and selectivity.

Introduction

Catalytic conversion of biomass and biomass derived platform compounds to biofuels and value-added chemicals attracts much attention in recent years.[1] Lactic acid (LA) and alkyl lactates are important chemicals that can be produced from biomass derived carbohydrates.[2] Glucose and sucrose are cheap and abundant materials for production of LA and alkyl lactates. Conversion of these hexoses to LA in water or to alkyl lactate in alcohol is a complex process including multiple steps.[3] Lewis acid catalyst shows particular activity and selectivity for production of LA and

View Article Online
DOI: 10.1039/C6GC02437H

alkyl lactate.[3] Compared to homogeneous Lewis acid,[3c,d,4] solid Lewis acid attracts much more interest due to its easy separation from the reaction mixture and recyclability.[3a,b,5] Sn-Beta zeolite is considered as the state-of-the-art catalyst for the conversion of C_6 carbohydrates to LA or alkyl lactate.[3a,5a,6] However, the hydrothermal synthesis of Sn-Beta is difficult, which usually needs fluoride as mineralizer, large amount of expensive tetraethyl ammonium hydroxide (TEAOH) as structure directing agent (SDA), and long crystallization time (generally more than 10 days).[3a,7] In addition, the crystal size of Sn-Beta synthesized in fluoride medium (Sn-Beta-F) is usually large, which would pose diffusion limitations on the catalytic reactions, especially the liquid reactions. It is reported that promoting the mass transfer is beneficial to improve the selectivity for LA and alkyl lactate.[6,8] Our recent work indicates that Sn-USY zeolite exhibits higher catalytic performance for the conversion of 1,3-dihydroxyacetone (DHA) to methyl lactate (MLA) than Sn-Beta-F due to its hierarchical porosity.[9] Unfortunately, the hierarchical Sn-USY zeolite prepared by the postsynthesis method gave poor selectivity for the conversion of C_6 carbohydrates to MLA. It is not a unique instance, but has its counterpart. The postsynthesized Sn-Beta zeolite also showed bad selectivity for MLA from the conversion of C_6 carbohydrates without the cocatalyst of alkali salts.[10] Due to the fact that the postsynthesis method is simple and scalable,[11] it is highly desirable to synthesize Sn-Beta zeolite by this method for efficient conversion of C_6 carbohydrates to alkyl lactates.

In the present work, a hydrothermal postsynthesis method with no fluoride and a

View Article Online
DOI: 10.1039/C6GC02437H

small amount of TEAOH is developed to prepare Sn-Beta zeolite, especially hierarchical Sn-Beta zeolite, for efficient conversion of C_6 carbohydrates to alkyl lactates. The method involves dealumination of Al-Beta zeolite to generate vacant T sites and mixing the dealuminated Beta (deAl-Beta) with Sn precursor through grinding, followed by a hydrothermal treatment of the mixture in the presence of low concentration of TEAOH (Scheme 1). The physicochemical properties of the hierarchical Sn-Beta zeolite were thoroughly characterized and its catalytic performance was investigated in the conversion of glucose to MLA in detail.

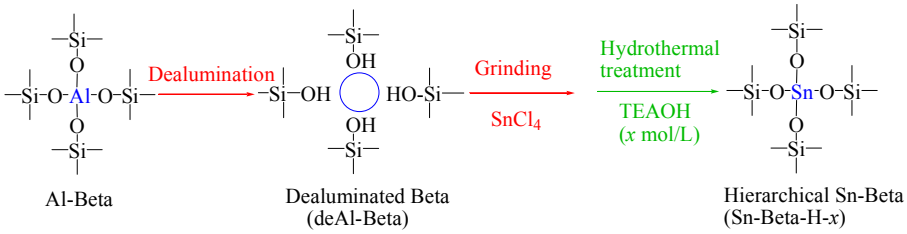

Scheme 1 Procedure for preparation of Sn-Beta-H zeolite.

Experimental section

Preparation of hierarchical Sn-Beta zeolites

The parent Al-Beta zeolite (Si/Al = 38.1, Nankai University Catalyst Co., China) was dealuminated with nitric acid (13 mol L^{-1}, 20 mL g^{-1} zeolite) at 100 ^{o}C for 20 h. After filtration and washing by water until the filtrate was neutral, the dealuminated zeolite was dried at 100 ^{o}C overnight. The aluminum content of deAl-Beta determined by ICP-AES is 0.03 wt% corresponding to Si/Al mole ratio of 1470. The dried deAl-Beta (0.5 g) was ground homogeneously with 0.03 g of $SnCl_4 \cdot 5H_2O$ (corresponding to nominal Sn content of 2 wt%), and then the mixture was hydrothermally treated with different concentration of TEAOH (10 mL g^{-1}) in a

View Article Online
DOI: 10.1039/C6GC02437H

stainless steel autoclave lined with polytetrafluorethylene. The treatment was performed at 140 ^{o}C for 24 h under static condition. The autoclave was quenched immediately in cool water and the solid was separated by centrifugation, washed with deionized water, dried at 100 ^{o}C, and calcined at 550 ^{o}C for 6 h in air, respectively. The treated samples were denoted as Sn-Beta-H-*x*, where *x* denotes the concentration of TEAOH.

As a reference, the calcined ground mixture of deAl-Beta and $SnCl_4 \cdot 5H_2O$ was given a name of Sn-Beta-P. Another reference sample, microporous Sn-Beta directly synthesized by the hydrothermal method in fluoride medium was denoted as Sn-Beta-F. The detailed synthesis process was given in Supporting Information.

Characterization of zeolites

Powder X-ray diffraction (XRD) was performed on a PANalytical X`pert PRO instrument with Cu Kα (λ = 0.15418 nm) radiation. Tube voltage and tube current were 40 kV and 40 mA, respectively. The crystallinities of the samples were calculated according to the intensity of the peaks at 2θ of 7.9^{o} and 22.9^{o}. The adsorption/desorption isotherms were measured with a Quantachrome Autosorb using N_2 as adsorbate at -196 ^{o}C. Samples were outgassed at 300 ^{o}C for 3 h prior to measurements. Total surface area was calculated based on Brunauer-Emmet-Taller (BET) method. Micropore size distributions were calculated according to Horvath-Kawazoe (HK) method, and mesopore size distributions were calculated from the desorption branch of the isotherm with Barret-Joyner-Halenda (BJH) method. Sn and Al content of zeolites was analyzed by induced coupled plasma-atomic

View Article Online
DOI: 10.1039/C6GC02437H

emission spectroscopy (ICP-AES) on an iCAP 6000 SERIES instrument. Ultraviolet-visible diffuse reflectance spectra (UV-vis DRS) were measured with an Agilent Technologies Cary Series UV-vis-NIR spectrophotometer. Scanning electron microscopy (SEM) was performed on JEOL JSM-6700F. Transmission electron microscopy (TEM) images were obtained on a Tecnai G2 F20 operated at 200 kV. Thermal analysis was performed on a NETZSCH STA 449F3 thermal analyzer under air atmosphere with a temperature ramp of 10 ^{o}C min^{-1}. Temperature programmed desorption of ammonia (NH_3-TPD) was measured on a homemade instrument. The sample was pretreated at 350 ^{o}C for 0.5 h in He, and then NH_3 was adsorbed at 100 ^{o}C. The desorption process was monitored with a TCD at a temperature ramp from 100 ^{o}C to 800 ^{o}C, with a heating rate of 10 ^{o}C min^{-1}. Fourier transform infrared (FT-IR) spectra of hydroxyl region and pyridine or deuterated acetonitrile (CD_3CN) adsorption were recorded on self-supporting wafers (~10 mg). After evacuated at 450 ^{o}C for 3 h, the wafers were cooled down to room temperature and the spectrum of hydroxyl region was acquired, which is also the background spectrum for pyridine or CD_3CN adsorption. Subsequently, pyridine or CD_3CN was adsorbed until saturation. The spectra of CD_3CN adsorption were scanned at room temperature per 5 min intervals. For the spectra of pyridine adsorption, the temperature was raised to the desired value and kept for 0.5 h. The spectrum was collected after the temperature was decreased again to room temperature.

Catalytic tests

A 10 mL stainless steel autoclave reactor was first charged with methanol (5 mL),

View Article Online
DOI: 10.1039/C6GC02437H

and then carbohydrate (0.124 g) and catalyst (80 mg) were added under stirring. After the autoclave was sealed, the atmosphere over the solution was replaced four times with N_2, and then the pressure was charged to 0.5 MPa. Subsequently, the reactor was heated to the desired temperature under stirring. When the reaction finished, it was quenched in ice-water bath, and the catalyst was separated by centrifugation. The products in the reaction solution were identified by an Agilent 6890N GC/5973 MS and a Shimadzu LC-20AT HPLC analysis system. Conversion of carbohydrate was analyzed with the external standard method on a Shimadzu LC-20AT HPLC analysis system equipped with an Aminex HPX-87H column (300 mm × 7.8 mm) and refractive index detector (RID-10A). 0.005 M aqueous H_2SO_4 was used as the mobile phase, which had a flow rate of 0.5 mL min^{-1}. The column temperature was 40 °C. MLA yield were analyzed on a GC equipped with an FID using naphthalene as the internal standard. Carbohydrate conversion and MLA yield were calculated as follows:

$$Carbohydrate\ conversion = \frac{moles\ of\ carbohydrate\ reacted}{moles\ of\ starting\ carbohydrate} \times 100\%$$

$$MLA\ yield = \frac{moles\ of\ MLA\ produced}{moles\ of\ starting\ carbohydrate} \times \frac{3}{N_C} \times 100\%$$

Where N_C is the number of carbon atoms in carbohydrate molecule.

For the recycling studies, the following procedure was adopted. After reaction in methanol at 160 ^oC for 10 h, the sample was centrifuged to deposit the solid catalyst. The recovered solid catalyst was washed three times with methanol, dried overnight at room temperature, calcined at 550 ^oC for 6 h, and then reused in the next reaction run.

View Article Online
DOI: 10.1039/C6GC02437H

Results and discussion

Synthesis of hierarchical Sn-Beta zeolite

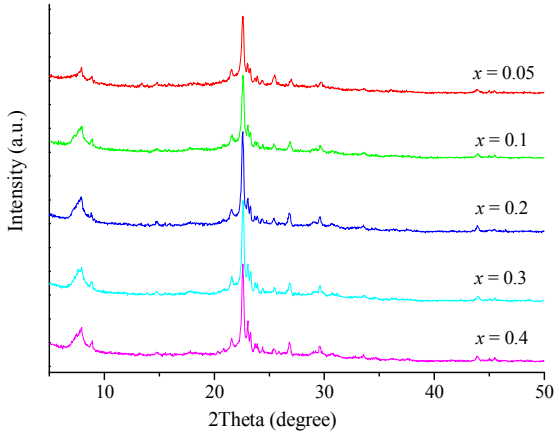

Fig. 1 XRD patterns of Sn-Beta-H-*x* (*x* represents the concentration of TEAOH.).

Table 1 Properties of Al-Beta, deAl-Beta and Sn-Beta zeolites

Sample	Sn content (wt%) (Si/Sn)[a]	S_{BET} (m^2 g^{-1})	Total pore volume (mL g^{-1})	External surface area (m^2 g^{-1})[b]	Mesopore volume (mL g^{-1})[b]	Crystallinity (%)[c]
Al-Beta	–	495	0.327	72	0.094	100
deAl-Beta	–	489	0.322	92	0.118	80
Sn-Beta-P	1.86 (104)	435	0.311	98	0.137	60
Sn-Beta-H-0.05	1.24 (157)	264	0.244	49	0.133	52
Sn-Beta-H-0.1	1.50 (129)	385	0.282	49	0.108	60
Sn-Beta-H-0.2	1.64 (118)	405	0.299	59	0.120	76
Sn-Beta-H-0.3	1.72 (112)	415	0.311	85	0.142	75
Sn-Beta-H-0.4	2.34 (82)	372	0.306	83	0.158	74

View Article Online
DOI: 10.1039/C6GC02437H

Sn-Beta-F	1.38 (140)	348	0.230	45	0.073	–

[a] Determined by ICP.

[b] External surface area = BET surface area – micropore surface area; mesopore volume = total pore volume – micropore volume, where micropore surface area and volume were determined by the *t*-plot method at a relative pressure of 0.05-0.70.

[c] Calculated according to the intensity of the peaks at 2θ of 7.9° and 22.9°.

The concentration of TEAOH plays a crucial role in the synthesis of hierarchical Sn-Beta zeolite. XRD patterns (Fig. 1) of Sn-Beta-H-*x* zeolites are similar with that of the parent zeolite, manifesting that the crystal phase preserved after hydrothermal treatment in the presence of TEAOH. SEM images (Fig. S1) revealed that both morphology and crystal size did not change obviously after hydrothermal treatment. The crystallinity of Sn-Beta-H-*x* decreased compared to deAl-Beta (Table 1), which is caused primarily by the mixing process via grinding. The relative crystallinity of Sn-Beta-P without hydrothermal treatment is only 60%. If taking Sn-Beta-P as a benchmark, the crystallinity of Sn-Beta-H-*x* decreased firstly and then increased with the enhancement in the concentration of TEAOH (Table 1). The crystallinity reached its maximum at the concentration of 0.2 mol L^{-1}. It is well known that TEAOH is a strong base, and also a frequently-used SDA for synthesis of Beta zeolites.[3a,7a,12] Therefore, the change in crystallinity with the concentration of TEAOH implies that, on the one hand, TEAOH acting as a strong base etched the structure of zeolite, and on the other hand TEAOH acting as a SDA reconstructed the structure of Beta zeolite.

View Article Online
DOI: 10.1039/C6GC02437H

The concentration of TEAOH is the key factor determining which one of the two opposite effects to be predominant during the hydrothermal treatment.

The results of N_2 physisorption (Table 1 and Fig. 2C) show that the BET surface area and the micropore volume of Sn-Beta-H-0.05 were much lower than Sn-Beta-P, which suggests that the structure of Sn-Beta-H-0.05 became partially amorphous by the etching of TEAOH. This is in agreement with the lowest crystallinity of Sn-Beta-H-0.05. The BET surface area and the micropore volume increased significantly with the increase in the concentration of TEAOH to 0.1 mol L^{-1}, indicating that the structure was reconstructed with the SDA. Further increasing the concentration of TEAOH, its etching effect became significant again. This was testified by the BJH-derived pore size distributions (Fig. 2B) and the increase of the mesopore volume and the external surface area (Table 1). The most probable mesopore diameter can be observed apparently at 7.8 nm for Sn-Beta-H-0.2, Sn-Beta-H-0.3, and Sn-Beta-H-0.4. The diameter of the mesopores is similar with the hierarchical Beta prepared by sequential desilication and dealumination.[13] TEM images (Fig. 3) confirm the formation of intracrystalline mesopores. The generation of these intracrystalline mesopores results from desilication of Beta zeolite, because the solid yield of Sn-Beta-H (Fig. 3D) decreased with the concentration of TEAOH. Similar result of organic base acting as desilication agent was also reported in literature.[14]

View Article Online
DOI: 10.1039/C6GC02437H

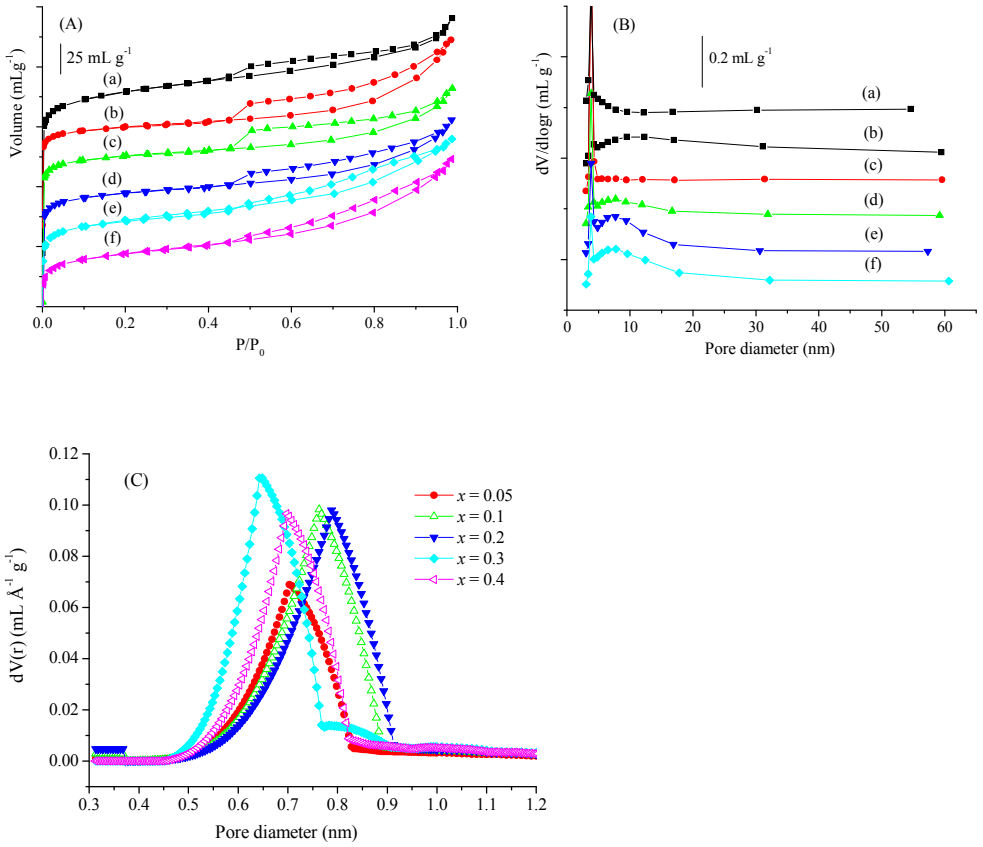

Fig. 2 N_2 isotherms (A), BJH (B) and HK (C) derived pore size distributions of (a) Sn-Beta-P and Sn-Beta-H-*x* (*x* represents the concentration of TEAOH.). (b) $x = 0.05$, (c) $x = 0.1$, (d) $x = 0.2$, (e) $x = 0.3$, (f) $x = 0.4$.

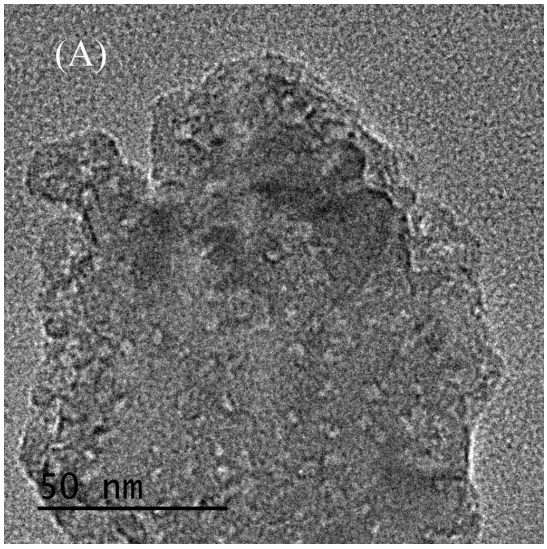

View Article Online
DOI: 10.1039/C6GC02437H

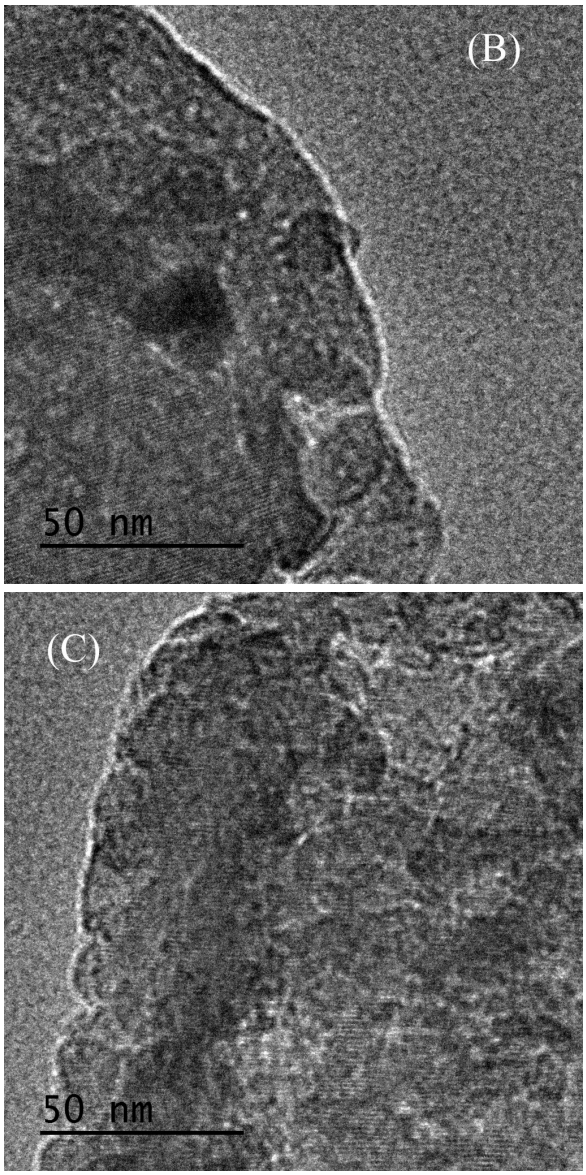

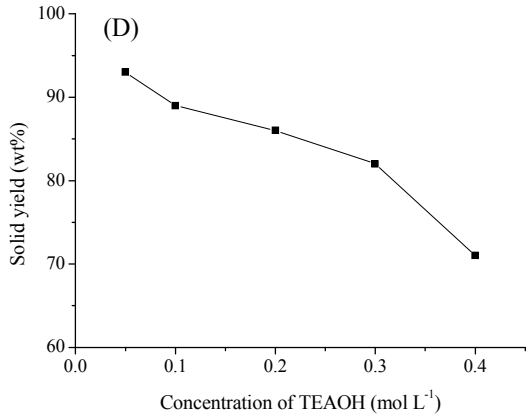

Fig. 3 TEM images of (A) Sn-Beta-H-0.2, (B) Sn-Beta-H-0.3 and (C) Sn-Beta-H-0.4,

View Article Online
DOI: 10.1039/C6GC02437H

and solid yield (D) of Sn-Beta-H-*x* after treatment with different concentration of TEAOH.

The crystalline framework of Sn-Beta-H-0.4 preserved well as shown above by the XRD results, though severe desilication took place at this point. This is one of the virtues of organic base as desilication agent;[14,15] in addition, TEAOH is a typical SDA for the synthesis of Beta zeolite, which is more favorable for preserving its BEA topology. If 0.3 mol L^{-1} NaOH was used as a desilication agent, it was found that the structure completely collapsed. During the hydrothermal treatment, the structure directing role of TEAOH was corroborated by the thermal analyses (Fig. 4A and Table S1). For Sn-Beta-H-*x*, three weight loss stages were observed from TG curves. The first stage (< 200 ^{o}C) is attributed to the desorption of water; the second one (200-350 ^{o}C) is ascribed to the oxidation and decomposition of TEA^{+}; the third one (> 350 ^{o}C) corresponds to removal of organic residue.[12] Sn-Beta-F showed similar oxidation-decomposition behaviors of TEAOH with Sn-Beta-H-*x*, confirming that TEAOH played structure directing role in the process of hydrothermal treatment. The total weight loss (Table S1) rose with the concentration of TEAOH until it reached 0.2 mol L^{-1}. The TG curves of Sn-Beta-H-0.2, Sn-Beta-H-0.3, and Sn-Beta-H-0.4 almost overlapped completely, implying that there is a fixed value for the amount of TEAOH as SDA to heal the defects of Sn-Beta-P. In general, the requisite amount of SDA for the synthesis of a zeolite is not random. Although deAl-Beta is already crystalline (Fig. S2), the crystallites have more silanol defects due to acid dealumination. As can be observed from the FT-IR spectra of the hydroxyl region (Fig. 4B), the absorption band

View Article Online
DOI: 10.1039/C6GC02437H

of hydroxyl groups at 3540 cm^{-1}, corresponding to the hydrogen-bonded internal silanols,[8c,16] enhanced dramatically after acid dealumination. This evidenced the formation of defect sites inside the framework. After hydrothermal treatment, the broad absorption band at 3540 cm^{-1} (Fig. 4B (d)) significantly decreased in intensity. The decrease is attributed to on the one hand the incorporation of Sn^{4+} occupying part defect sites, because the intensity of this absorption band for Sn-Beta-P (Fig. 4B (c)) without hydrothermal treatment also reduced obviously; on the other hand TEAOH interacted with and healed up some defect sites, resulting to further decrease of the defect sites. However, the defect sites of Sn-Beta-H-0.3 are still more than that of Sn-Beta-F synthesized in fluoride medium, which is considered to be defect-free.[17]

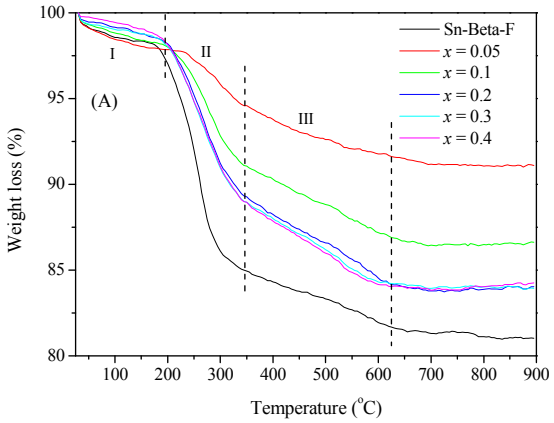

View Article Online
DOI: 10.1039/C6GC02437H

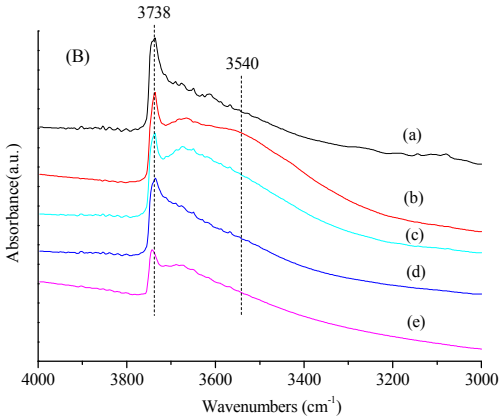

Fig. 4 TG analyses (A) of Sn-Beta-H-*x* and Sn-Beta-F, and FT-IR spectra (B) of the hydroxyl region of (a) Al-Beta, (b) deAl-Beta, (c) Sn-Beta-P, (d) Sn-Beta-H-0.3 and (e) Sn-Beta-F.

Content and state of Sn in hierarchical Sn-Beta zeolite

The framework Sn species are the active centers of stannosilicate zeolites as catalysts,[18] so the content and state of Sn in the hierarchical Sn-Beta zeolites was determined. The content of Sn in Sn-Beta-H-*x* was affected by the concentration of TEAOH (Table 1), which gradually advanced with the concentration of TEAOH; but the content of Sn in Sn-Beta-H-*x* was lower than that in Sn-Beta-P when the concentration of TEAOH was lower than 0.4 mol L^{-1}. This indicates that a fraction of Sn entered the aqueous solution during the hydrothermal treatment. The content of Sn in Sn-Beta-H-0.4 was higher than that in Sn-Beta-P due to severe desilication by TEAOH as observed in Fig. 3D.

UV-vis DR spectroscopy and FT-IR spectroscopy of CD_3CN adsorption were employed to further reveal the state of Sn in Sn-Beta-H, although the above FT-IR spectra of the hydroxyl region provide the information of Sn incorporation into the

View Article Online
DOI: 10.1039/C6GC02437H

vacant framework sites. UV-vis DR spectra in Fig. 5A show that both Sn-Beta-P and Sn-Beta-H-0.3 exhibit a band at 200 nm, which is ascribed to the charge transfer of O^{2-} to Sn^{4+} in the framework positions.[13,19] The intensity of this band for Sn-Beta-H-0.3 is higher than that of Sn-Beta-P though the content of Sn in both samples is comparable, suggesting that more isolated tetrahedrally coordinated Sn^{4+} species were formed.[20] Nevertheless, a small amount of Sn species present at extraframework sites is not excluded. CD_3CN adsorption is a powerful tool to identify the isolated framework metal sites, which interacts with tetrahedrally coordinated framework Sn sites and displays a characteristic absorbance in IR spectrum at ~2311 cm^{-1}.[9,13,16] Indeed, the hierarchical Sn-Beta-H-0.3 shows an absorbance at 2310 cm^{-1} (Fig. 5B), explicitly demonstrating that Sn was incorporated into the framework sites.

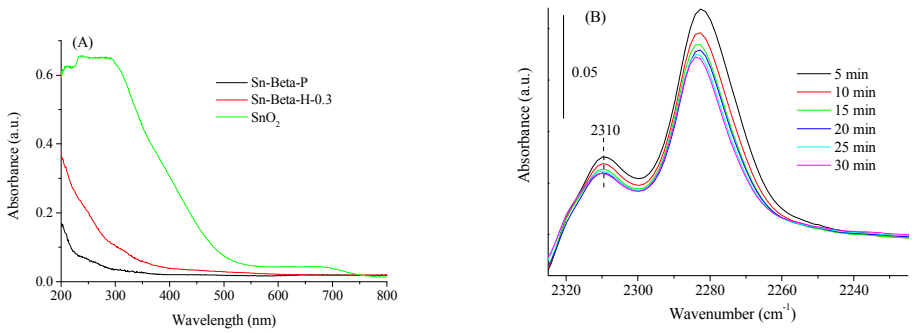

Fig. 5 UV-Vis DRS (A) of Sn-Beta-H-0.3, Sn-Beta-P and SnO_2, and FT-IR spectra (B) of CD_3CN adsorbed on Sn-Beta-H-0.3 (The spectra were measured after saturation of CD_3CN on the samples followed by different desorption times at 25 ^oC.).

Acidity of hierarchical Sn-Beta zeolite

The acidity of Sn-Beta-H-0.3 was monitored with NH_3-TPD and FT-IR spectroscopy of pyridine adsorption measurements. FT-IR spectra of adsorbed

View Article Online
DOI: 10.1039/C6GC02437H

pyridine of Sn-Beta-H-0.3 (Fig. 6A) exhibit two strong absorption bands at 1452 cm^{-1} and 1612 cm^{-1} corresponding to pyridine adsorbed on Lewis acid sites.[20a,21] FT-IR spectra of pyridine adsorbed on deAl-Beta (Fig. S3) do not show these characteristic absorption bands, which suggests that the Lewis acid sites of Sn-Beta-H-0.3 were generated by Sn incorporation. A weak band at ~1547 cm^{-1} representing pyridine adsorbed on Brønsted acid sites is observed for both Sn-Beta-H-0.3 and deAl-Beta, meaning that the Brønsted acid sites originate from the small amount of residual framework Al (0.03 wt%). These results suggest that Sn-Beta-H-0.3 mainly comprise Lewis acid sites, like other Sn-Beta zeolites reported in literature.[20] The Lewis acid density of Sn-Beta-H-0.3 was calculated based on the peak at 1452 cm^{-1} according to the equation given in literature,[22] and compared with that of Sn-Beta-F (Fig. S4). It can be seen from Table S2 that the Lewis acid density for both samples is comparable. NH_3-TPD (Fig. 6B) result indicates that there is an intense desorption peak at temperature lower than 350 ^oC, corresponding to weak acid sites. Another desorption peak is also observed at 490 ^oC which is related to strong acid sites.[23] This means Sn located in different micro-environments. Additionally, Sn-Beta-H-0.3 comprises less strong acid sites than Sn-Beta-F.

View Article Online
DOI: 10.1039/C6GC02437H

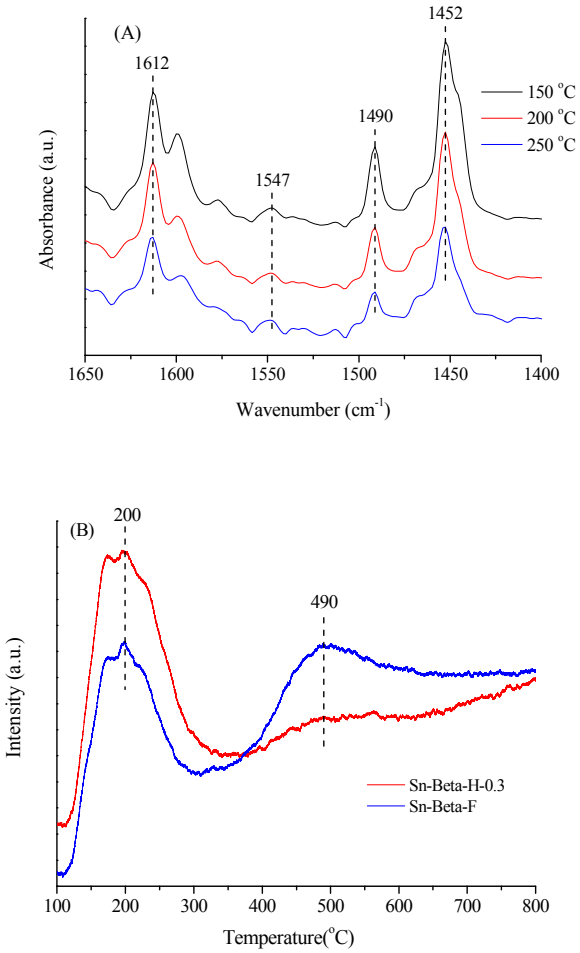

Fig. 6 FT-IR spectra (A) of adsorbed pyridine of Sn-Beta-H-0.3, and NH_3-TPD curves (B) of Sn-Beta-H-0.3 and Sn-Beta-F.

Catalytic performance of hierarchical Sn-Beta zeolite

View Article Online
DOI: 10.1039/C6GC02437H

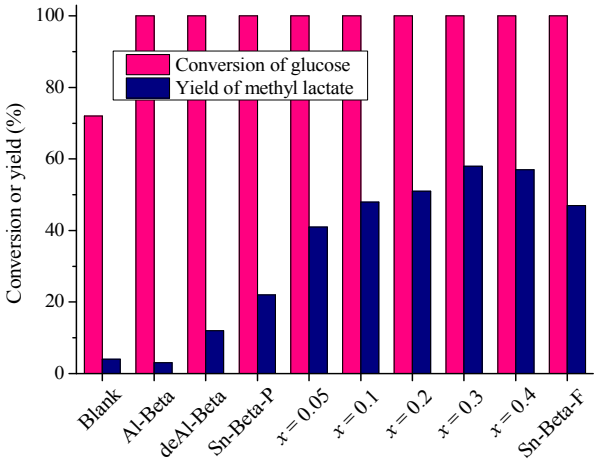

Fig. 7 Conversion of glucose in methanol over various Beta zeolites. Reaction conditions: 0.124 g glucose, 80 mg catalyst, 5 mL methanol, 0.5 MPa N_2, 160 ^oC, 10 h.

The catalytic performance of Sn-Beta-H-*x* was tested in the conversion of glucose to MLA in methanol (Fig. 7). For comparison, the catalytic performance of Al-Beta, deAl-Beta, Sn-Beta-P and Sn-Beta-F was also investigated. Glucose was completely converted over all tested catalysts except the blank reaction. The yield of MLA was 22% over Sn-Beta-P, which was consistent with that reported in literature.[10] Over Sn-Beta-H-*x*, the yield of MLA was remarkably enhanced. Moreover, the yield of MLA increased gradually with the concentration of TEAOH until it reached 0.3 mol L^{-1}. 58% of MLA yield was acquired over Sn-Beta-H-0.3, which is higher than that over Sn-Beta-F (47%). It is widely accepted that the reaction route for the conversion of glucose to MLA (Scheme S1) contains: (1) isomerization of glucose to fructose, (2) retro-aldol of fructose to DHA and glyceraldehyde (GLA), and (3) isomerization of DHA and GLA to MLA.[3,5b] The second step is considered as the rate-determining

View Article Online
DOI: 10.1039/C6GC02437H

step,[3a,24] and Lewis acid sites related to framework Sn^{4+} in stannosilicate are efficient active sites for this reaction.[3a] Due to the fact that the crystal size, the content and state of Sn and the acidity of Sn-Beta-H-0.3 and Sn-Beta-F are similar, the difference in the catalytic performance can be attributed to the different porosity. In order to investigate the promotion effect of the hierarchical pores on the rate-determining step, Sn-Beta-H-0.3 was tested for the conversion of fructose in methanol and compared with Sn-Beta-F. A lower temperature (120 ^{o}C) was selected in order to observe the intermediate products of this reaction and at the same time compare conveniently the performance of Sn-Beta-H-0.3 and Sn-Beta-F for the retro-aldol reaction of fructose. For the conversion of fructose to C_3 compounds, Sn-Beta-H-0.3 gave 71% of yield of total C_3 derivatives, whereas Sn-Beta-F only gave 42% (Table 2). The pseudo-yield of retro-aldol reaction of fructose (Table S3) over Sn-Beta-H-0.3 was calculated according to the formula reported in literature,[4c] which was twice as high as that over Sn-Beta-F. Kinetic analyzing results (Fig. S5 and Fig. S6) showed that the retro-aldol reaction fitted well with the pseudo-first-order reaction kinetics, which is consistent with that reported for the retro-aldol reaction of glucose.[25] The apparent activation energy over Sn-Beta-H-0.3 and Sn-Beta-F is 100, and 96 kJ mol^{-1}, respectively (Fig. S7). The values are lower than that for the retro-aldol reaction of glucose over ammonium metatungstate.[26] In addition, Sn-Beta-H-0.3 shows a rate constant for the retro-aldol reaction of fructose twice higher than Sn-Beta-F at the same temperature, though the activation energy over Sn-Beta-H-0.3 and Sn-Beta-F is comparable. These results clearly prove that Sn-Beta-H-0.3 possesses much higher catalytic activity

View Article Online
DOI: 10.1039/C6GC02437H

toward the retro-aldol reaction of fructose to C_3 sugars. The retro-aldol reaction of fructose to C_3 sugars involved activation of oxygen atom on C2 and C4 by one Sn site and formation of a six-membered ring.[6,26] The hierarchical pores probably facilitated to reduce steric hindrance of the hydromethyl group (C1) of the transition states for the retro-aldol reaction, and make it proceed smoothly. Thus, the yield of MLA was increased.

Table 2 Conversion of fructose over Sn-Beta-H-0.3 and Sn-Beta-F in methanol[a]

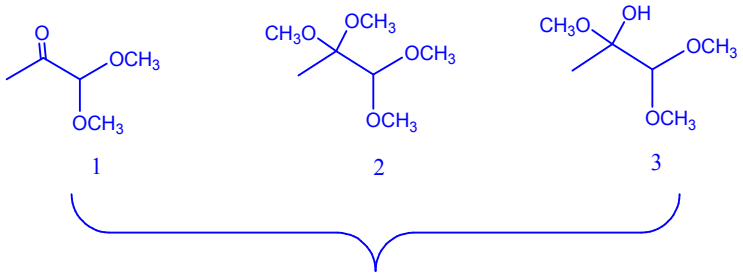

		Yield (%)					
Catalyst	Conversion of fructose (%)	MLA	Compound 1	Compound 2	Compound 3	Total C_3 compounds	
Sn-Beta-H-0.3	95	41	2	18	10	71	
Sn-Beta-F	84	22	3	10	7	42	

[a] Reaction conditions: 0.248 g fructose, 0.160 g catalyst, 10 mL methanol, 0.5 MPa N_2, 120 ^{o}C, 1 h.

Higher alcohols including ethanol and *n*-butanol were also employed as solvents. The yields of corresponding alkyl lactate were 41% and 29%, respectively, which are

View Article Online
DOI: 10.1039/C6GC02437H

comparable to the yields reported in literature with sucrose as substrate.[3a] The catalytic performance of Sn-Beta-H-0.3 was also tested for the conversion of other carbohydrates (Table 3). Sn-Beta-H-0.3 is active for converting all of the studied carbohydrates. The yield of MLA with 1,3-dihydroxyacetone (DHA) as substrate (entry 3) was the highest due to the easiest conversion of triose compared to hexose. The yields of MLA from fructose and mannose (entries 4 and 5) were comparable to that from glucose, because Lewis acid Sn-Beta can catalyze the isomerization between these sugars.[5a] Sucrose, a disaccharide composed of glucose and fructose units, gave slightly lower MLA yield than monosaccharides; probably the presence of glycosidic bond restrains its conversion. With the pentose of xylose being used as the substrate, 53% of MLA yield was obtained (entry 7).

Table 3 Conversion of carbohydrates to alkyl lactate over Sn-Beta-H-0.3[a]

Entry	Substrate	Solvent	Conversion (%)	Yield of alkyl lactate (%)
1	Glucose	Ethanol	100	41
2	Glucose	*n*-Buthanol	100	29
3[b]	DHA	Methanol	>99	89
4	Fructose	Methanol	100	55
5	Mannose	Methanol	100	54
6	Sucrose	Methanol	100	50
7	Xylose	Methanol	100	53

[a] Reaction conditions: 0.124 g carbohydrate, 80 mg catalyst, 5 mL methanol, 0.5 MPa

View Article Online
DOI: 10.1039/C6GC02437H

N_2, 160 ^oC, 10 h.

[b] The reaction temperature and time for DHA conversion were 90 ^oC and 5 h, respectively.

The catalytic performance of Sn-Beta zeolites prepared by the hydrothermal postsynthesis method is independent on the properties of the parent Al-Beta. Starting from two other Al-Beta zeolites with Si/Al ratio of 19.5 and 13.8, the obtained Sn-Beta-H-*x* gave similar yields of MLA from glucose (Table S4). In addition, keeping the concentration of TEAOH at 0.3 mol L^{-1} and increasing the ratio of zeolite to TEAOH solution from 1/10 to 1/5 (g mL^{-1}) did not influence the catalytic performance of the catalyst (Table S4, entry 8). At this point, the consumption amount of TEAOH only accounts for 17% of that used in the hydrothermal synthesis of Sn-Beta-F. This is significant for saving cost and diminishing environmental pollution.

Reusability of hierarchical Sn-Beta zeolite

The hydrothermal postsynthesis method for preparation of the hierarchical Sn-Beta without using toxic fluoride and only consuming a small amount of TEAOH is more environmentally friendly and economical than the traditional hydrothermal synthesis method. Finally, the stability and the recyclability of the hierarchical Sn-Beta were investigated, which are important for a heterogeneous catalyst besides the catalytic activity and the selectivity. As shown in Fig. 8, the conversion of glucose was complete, and the yield of MLA only decreased slightly and remained as high as 48% after five consecutive reaction runs. It was observed that the color of the catalyst

View Article Online
DOI: 10.1039/C6GC02437H

gradually became deep after every recycling and turned to light gray after five recyclings even after calcination at 550 ^{o}C for 6 h (Fig. S8), while the crystalline structure of Sn-Beta-H-0.3 kept well (Fig. S9). So, the fouling of the catalyst should account for the slight decrease of the catalytic performance during recycling.

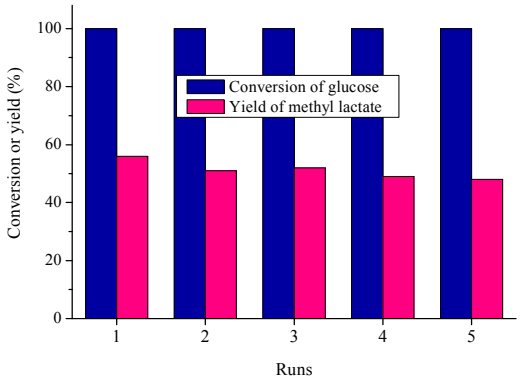

Fig. 8 Reusing test of Sn-Beta-H-0.3 in the conversion of glucose to MLA. Reaction conditions: 0.372 g glucose, 0.240 g catalyst, 15 mL methanol solution, 0.5 MPa N_2, 160 ^{o}C, 10 h.

Conclusions

In conclusion, a hydrothermal postsynthesis method was developed successfully to prepare hierarchical Sn-Beta zeolite, which involves dealumination to generate vacant T sites, mixing dealuminated Beta with $SnCl_4$, and then hydrothermal treatment in the presence of TEAOH. During hydrothermal treatment, TEAOH plays dual roles; one is acting as a base to desilicate and the other is as a SDA to preserve the structure of Beta. The concentration of TEAOH determined which one of the two roles to be predominant. Hierarchical Sn-Beta with 7.8 nm mesopores can be obtained at the concentration of 0.2~0.4 mol L^{-1}. The hierarchical Sn-Beta exhibits higher catalytic

View Article Online
DOI: 10.1039/C6GC02437H

performance in the conversion of glucose to MLA than the conventional Sn-Beta synthesized in fluoride medium, which remarkably promotes the rate-determining step of retro-aldol of fructose and thus the yield of MLA.

Acknowledgements

We are grateful to the NSFC-Henan Joint Foundation (U1304209) and the Outstanding Young Talent Research Fund of Zhengzhou University (1521316006) for the financial supports. Financial supports from the National Natural Science Foundation of China (J1210060) and the Undergraduate Innovative Training Program of Zhengzhou University (2016xjxm266) are also acknowledged.

Reference

1 (a) M. Yabushita, H. Kobayashia and A. Fukuoka, *Appl. Catal. B: Environ.*, 2014, **145**, 1–9; (b) R. Rinaldi and F. Schüth, *Energy Environ. Sci.*, 2009, **2**, 610–626; (c) L. E. Manzer, *Top. Catal.*, 2010, **53**, 1193–1196; (d) P. C. A. Bruijnincx and Y. Román-Leshkov, *Catal. Sci. Technol.*, 2014, **4**, 2180–2181.

2 (a) A. Corma, S. Iborra and A. Velty, *Chem. Rev.*, 2007, **107**, 2411-2502; (b) M. Dusselier, P. V. Wouwe, A. Dewaele, E. Makshina and B. F. Sels, *Energy Environ. Sci.*, 2013, **6**, 1415–1442; (c) P. Mäki-Arvela, I. L. Simakova, T. Salmi and D. Yu. Murzin, *Chem. Rev.*, 2014, **114**, 1909–1971.

3 (a) M. S. Holm, S. Saravanamurugan and E. Taarning, *Science*, 2010, **328**, 602–605; (b) W. Dong, Z. Shen, B. Peng, M. Gu, X. Zhou, B. Xiang and Y. Zhang, *Sci. Rep.*, 2016, 6:26713, DOI: 10.1038/srep26713; (c) Z. Tang, W. Deng, Y. Wang, E. Zhu, X. Wan, Q. Zhang and Y. Wang, *ChemSusChem*, 2014, **7**, 1557–1567; (d) L. Zhou, L.

View Article Online
DOI: 10.1039/C6GC02437H

Wu, H. Li, X. Yang, Y. Su, T. Lu and J. Xu, *J. Mol. Catal. A*, 2014, **388–389**, 74–80.

4 (a) X. Lei, F. Wang, C. Liu, R. Yang and W. Dong, *Appl. Catal. A: Gen.*, 2014, **482**, 78–83; (b) F. Wang, C. Liu and W. Dong, *Green Chem.*, 2013, **15**, 2091–2095; (c) K. Nemoto, Y. Hirano, K. Hirata, T. Takahashi, H. Tsuneki, K. Tominaga and K. Sato, *Appl. Catal. B: Environ.*, 2016, **183**, 8–17; (d) Y. Wang, W. Deng, B. Wang, Q. Zhang, X. Wan, Z. Tang, Y. Wang, C. Zhu, Z. Cao, G. Wang and H. Wan, *Nature Commun.*, 2013, 4:2141, DOI: 10.1038/ncomms3141; (e) Z. Huo, Y. Fang, D. Ren, S. Zhang, G. Yao, X. Zeng and F. Jin, *ACS Sustainable Chem. Eng.*, 2014, **2**, 2765–2771.

5 (a) M. S. Holm, Y. J. Pagán-Torres, S. Saravanamurugan, A. Riisager, J. A. Dumesic and E. Taarning, *Green Chem.*, 2012, **14**, 702–706; (b) F. de Clippel, M. Dusselier, R. V. Rompaey, P. Vanelderen, J. Dijkmans, E. Makshina, L. Giebeler, S. Oswald, G. V. Baron, J. F. M. Denayer, P. P. Pescarmona, P. A. Jacobs and B. F. Sels, *J. Am. Chem. Soc.*, 2012, **134**, 10089–10101; (c) B. Murillo, B. Zornoza, O. de la Iglesia, C. Téllez and J. Coronas, *J. Catal.*, 2016, **334**, 60–67; (d) Q. Guo, F. Fan, E. A. Pidko, W. N. P. van der Graaff, Z. Feng, C. Li and E. J. M. Hensen, *ChemSusChem*, 2013, **6**, 1352–1356; (e) L. Yang, X. Yang, E. Tian, V. Vattipalli, W. Fan and H. Lin, *J. Catal.*, 2016, **333**, 207–216; (f) F. Wang, J. Liu, H. Li, C. Liu, R. Yang and W. Dong, *Green Chem.*, 2015, **17**, 2455–2463.

6 C. M. Osmundsen, M. S. Holm, S. Dahl and E. Taarning, *Proc. R. Soc. A*, 2012, **468**, 2000–2016.

View Article Online
DOI: 10.1039/C6GC02437H

7 (a) S. Tolborg, A. Katerinopoulou, D. D. Falcone, I. Sádaba, C. M. Osmundsen, R. J. Davis, E. Taarning, P. Fristrup and M. S. Holm, *J. Mater. Chem. A*, 2014, **2**, 20252–20262; (b) A. Corma, L. T. Nemeth, M. Renz and S. Valencia, *Nature*, 2001, **412**, 423–425; (c) Y. Román-Leshkov, M. Moliner, J. A. Labinger and M. E. Davis, *Angew. Chem. Int. Ed.*, 2010, **49**, 8954–8957; (d) C. M. Lew, N. Rajabbeigi and M. Tsapatsis, *Microporous Mesoporous Mater.*, 2012, **153**, 55–58.

8 (a) R. M. West, M. S. Holm, S. Saravanamurugan, J. Xiong, Z. Beversdorf, E. Taarning and C. H. Christensen, *J. Catal.*, 2010, **269**, 122–130; (b) H. Je Cho, P. Dornath and W. Fan, *ACS Catal.*, 2014, **4**, 2029–2037; (c) P. Y. Dapsens, C. Mondelli, J. Jagielski, R. Hauert and J. Pérez-Ramírez, *Catal. Sci. Technol.*, 2014, **4**, 2302–2311.

9 X. Yang, L. Wu, Z. Wang, J. Bian, T. Lu, L. Zhou, C. Chen and J. Xu, *Catal. Sci. Technol.*, 2016, **6**, 1757–1763.

10 S. Tolborg, I. Sádaba, C. M. Osmundsen, P. Fristrup, M. S. Holm and E. Taarning, *ChemSusChem*, 2015, **8**, 613–617.

11 C. Hammond, S. Conrad and I. Hermans, *Angew. Chem. Int. Ed.*, 2012, **51**, 1–5.

12 Z. He, J. Wu, B. Gao and H. He, *ACS Appl. Mater. Interfaces*, 2015, **7**, 2424–2432.

13 A. Al-Nayili, K. Yakabi and C. Hammond, *J. Mater. Chem. A*, 2016, **4**, 1373–1382.

14 (a) M. S. Holm, M. K. Hansen and C. H. Christensen, *Eur. J. Inorg. Chem.*, **2009**, 1194–1198; (b) J. Zhou, J. Teng, L. Ren, Y. Wang, Z. Liu, W. Liu, W. Yang and Z. Xie, *J. Catal.*, 2016, **340**, 166–176.

15 (a) J. Pérez-Ramírez, D. Verboekend, A. Bonilla and S. Abelló, *Adv. Funct. Mater.*,

View Article Online
DOI: 10.1039/C6GC02437H

2009, **19**, 3972–3979; (b) K. Sadowska, K. Góra-Marek, M. Drozdek, P. Kuśtrowski, J. Datka, J. Martinez Triguero and F. Rey, *Microporous Mesoporous Mater.*, 2013, **168**, 195–205; (c) K. Sadowska, A. Wach, Z. Olejniczak, P. Kuśtrowski and J. Datka, *Microporous Mesoporous Mater.*, 2013, **167**, 82–88.

16 P. Wolf, C. Hammond, S. Conrad and I. Hermans, *Dalton Trans.*, 2014, **43**, 4514–4519.

17 R. Gounder and M. E. Davis, *AIChE J.*, 2013, **59**, 3349–3358.

18 (a) P. Y. Dapsens, C. Mondelli and J. Pérez-Ramírez, *Chem. Soc. Rev.*, 2015, **44**, 7025-7043; (b) M. Moliner, *Dalton Trans.*, 2014, **43**, 4197–4208.

19 (a) J. Jin, X. Ye, Y. Li, Y. Wang, L. Li, J. Gu, W. Zhao and J. Shi, *Dalton Trans.*, 2014, **43**, 8196–8204; (b) B. Tang, W. Dai, X. Sun, G. Wu, N. Guan, M. Hunger and L. Li, *Green Chem.*, 2015, **17**, 1744–1755; (c) J. Dijkmans, D. Gabriëls, M. Dusselier, F. de Clippel, P. Vanelderen, K. Houthoofd, A. Malfliet, Y. Pontikes and B. F. Sels, *Green Chem.*, 2013, **15**, 2777–2785; (d) J. Dijkmans, M. Dusselier, D. Gabriëls, K. Houthoofd, P. Magusin, S. Huang, Y. Pontikes, M. Trekels, A. Vantomme, L. Giebeler, S. Oswald and B. F. Sels, *ACS Catal.*, 2015, **5**, 928–940.

20 (a) P. Li, G. Liu, H. Wu, Y. Liu, J. Jiang and P. Wu, *J. Phys. Chem. C*, 2011, **115**, 3663–3670; (b) J. Dijkmans, J. Demol, K. Houthoofd, S. Huang, Y. Pontikes and B. Sels, *J. Catal.*, 2015, **330**, 545–557.

21 (a) C. Chang, H. Je Cho, Z. Wang, X. Wang and Wei Fan, *Green Chem.*, 2015, **17**, 2943–2951; B. Tang, W. Dai, G. Wu, N. Guan, L. Li and M. Hunger, *ACS Catal.*, 2014, **4**, 2801−2810; (c) W. N. P. van der Graaff, G. Li, B. Mezari, E. A. Pidko and

View Article Online
DOI: 10.1039/C6GC02437H

E. J. M. Hensen, *ChemCatChem*, 2015, **7**, 1152–1160.

22 J. W. Harris, M. J. Cordon, J. R. Di Iorio, J. C. Vega-Vila, F. H. Ribeiro, R. Gounder, *J. Catal.*, 2016, **335**, 141–154.

23 M. P. Pachamuthu, K. Shanthi, R. Luque and A. Ramanathan, *Green Chem.*, 2013, **15**, 2158–2166.

24 M. Orazov and M. E. Davis, *PNAS*, 2015, **112**, 11777–11782.

25 J. Zhang, B. Hou, A. Wang, Z. Li, H. Wang and T. Zhang, *AIChE J.*, 2014, **60**, 3804–3813.

26 (a) P. Singh, A. Kumar, S. Kaur and A. Singh, *Org. Biomol. Chem.*, 2015, **13**, 4210–4220; (b) R. S. Assary and L. A. Curtiss, *Energy Fuels*, 2012, **26**, 1344−1352.

View Article Online
DOI: 10.1039/C6GC02437H

Hierarchical Sn-Beta zeolite was prepared by a hydrothermal postsynthesis method. It shows high catalytic activity for the conversion of glucose to alkyl lactate, which is better compared to microporous Sn-Beta synthesized by traditional hydrothermal method in fluoride media.

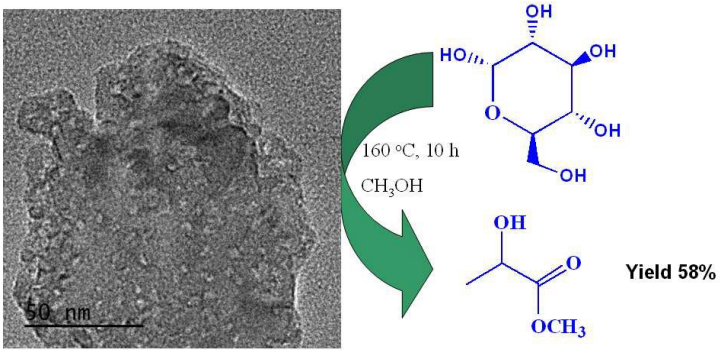

Hierarchical Sn-Beta